

Supplementary information for

Understanding of binding energy calibration in XPS of lanthanum oxide by in situ treatment

Jerry Pui Ho Li ^a, Xiaohong Zhou ^a, Yaoqi Pang^a, Liang Zhu ^a, Evgeny I. Vovk ^a, Linna Cong^a, Alexander P. van Bavel ^b, Shenggang Li^a, Yong Yang ^a

^a School of Physical Science and Technology, ShanghaiTech University, 100 Haik Road, Shanghai, 201210, China

^b Shell Global Solutions International B.V., Amsterdam, 1031 CM, The Netherlands

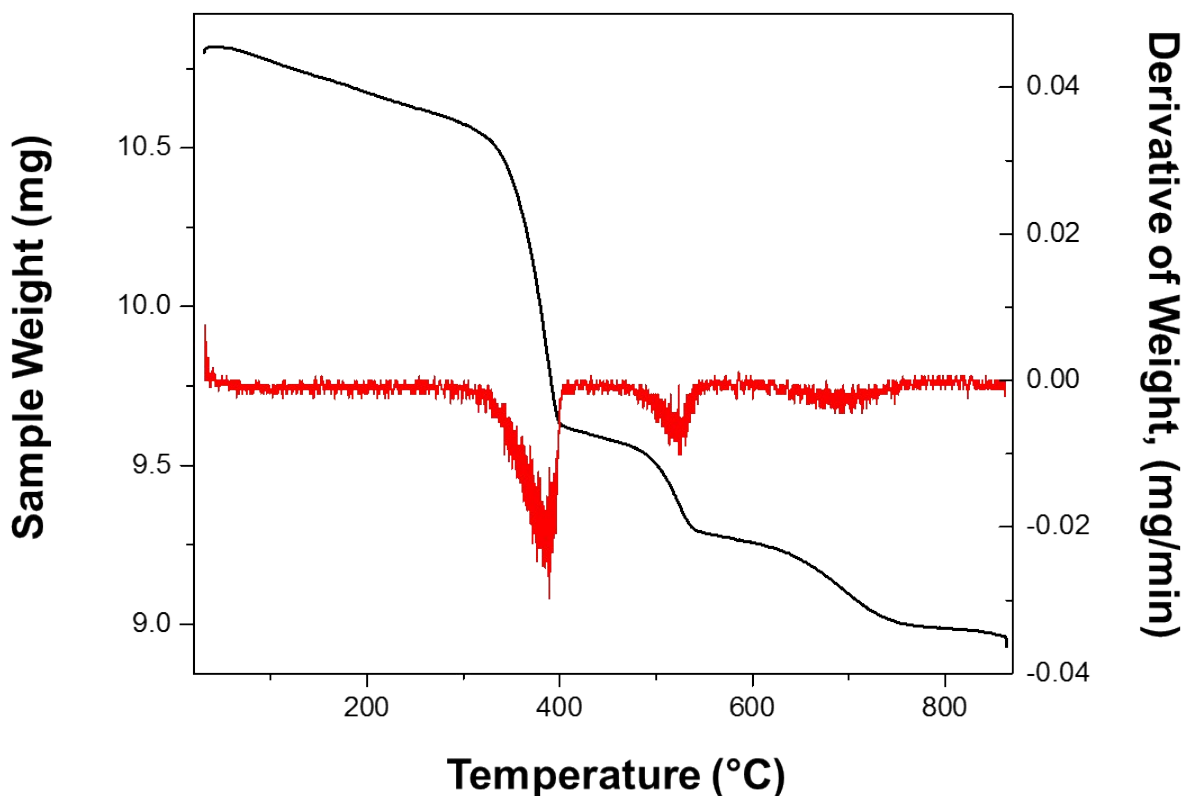


Figure S1. Thermogravimetric analysis (TGA) (black) and derivative weight loss curves (red) of La_2O_3 sample under N_2 flow

TGA results show that 3 steps of mass change are observed after 100°C. In the 1st step, a 10 % mass loss was observed at ~380°C identified as H_2O desorption. In the 2nd step, a 2.7 % mass loss was observed at ~510°C identified as additional H_2O desorption. Finally, in the 3rd step, a 2.7 % mass loss was observed at ~700°C identified as CO_2 desorption. As the desorption species are confirmed with the MS signal obtained. The results are also in line with the literature ^{1, 2}. It has been reported that in the 1st step, a mixture of $\text{La}_2(\text{OH})_4(\text{CO}_3)$ and $\text{La}(\text{OH})_3$ phases are decomposed to form $\text{La}_2\text{O}_2\text{CO}_3$ and LaOOH respectively, both yielding H_2O as desorbed product. The 2nd step is the subsequent LaOOH decomposition to La_2O_3 , yielding additional H_2O as desorbed product. The 3rd step is $\text{La}_2\text{O}_2\text{CO}_3$ phase being decomposed to La_2O_3 yielding CO_2 as the desorbed product ³.

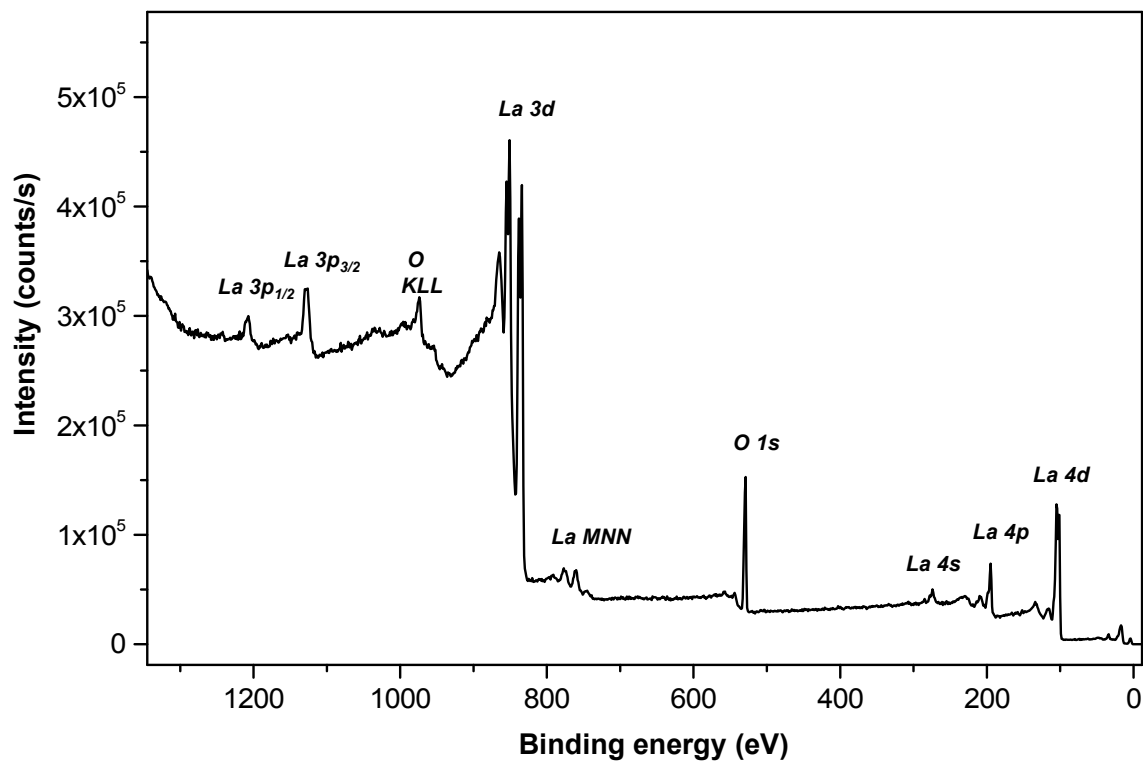


Figure S2. XPS survey scan of clean La_2O_3 surface (after 800°C calcination in HPGS of XPS spectrometer).

La 4p_{3/2} spectra of La_2O_3 sample taken after different treatments are shown in Figure S3. The binding energy scale is calibrated to La 4d_{5/2} peak at 102.2 eV as described in the main text. On treatments La 4p_{3/2} peak (195.7 eV) demonstrates no variation (± 0.05 eV) which makes this peak an alternative internal standard for calibration even if it two times less intense than La 4d_{3/2} peak.

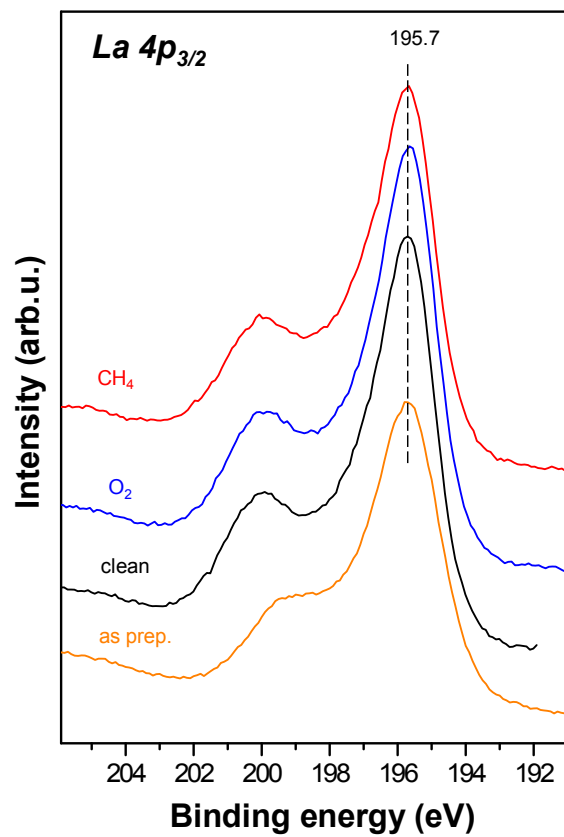


Figure S3. La 4p_{3/2} core level spectra of as prepared La₂O₃ surface (brown), clean surface after 800°C in situ calcination (black), and after interaction with O₂ (blue) and CH₄ (red).

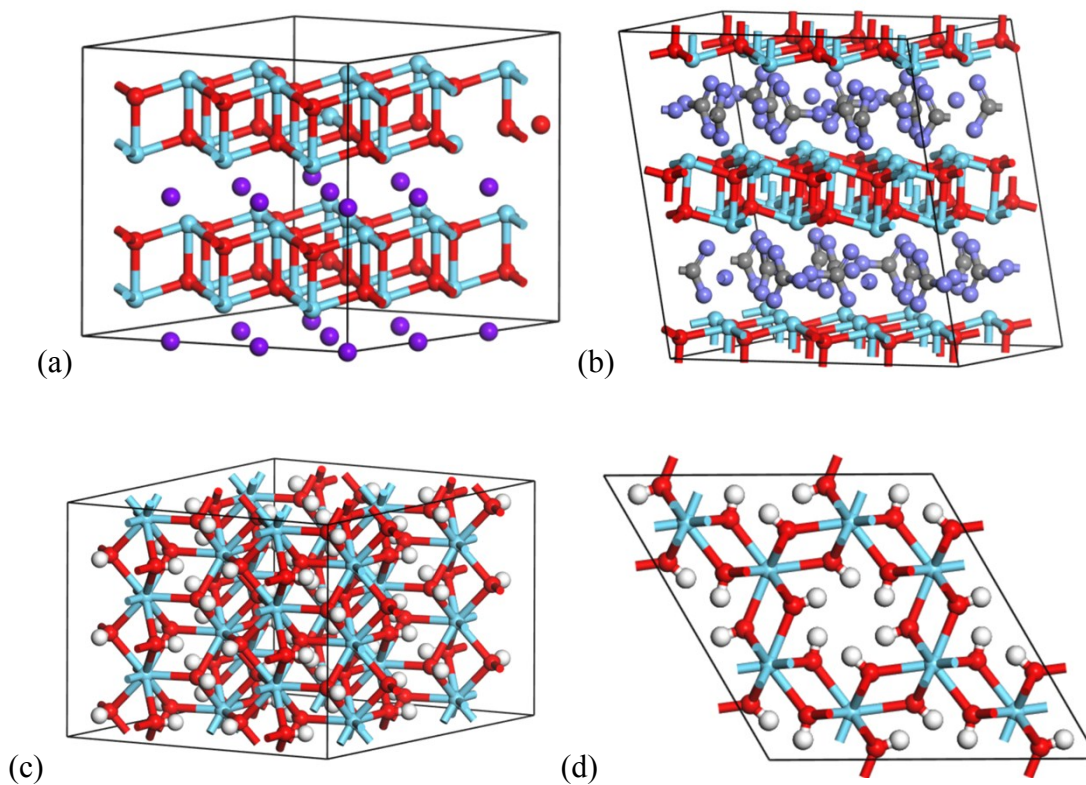


Figure. S4. (a) The (3x3x3) supercell of bulk La_2O_3 . Blue: lanthanum atom; Red: four-coordinated oxygen (O_{4c}); Purple: six-coordinated oxygen (O_{6c}). (b) The (2x2x1) supercell of bulk $\text{La}_2\text{O}_2\text{CO}_3$. Blue: lanthanum atom; Grey: carbon atom; Light purple: oxygen atom in the carbonate species; Red: non-carbonate oxygen atom (O_{4c}). (c) The (2x2x3) supercell of bulk $\text{La}(\text{OH})_3$. Blue: lanthanum atom; Red: oxygen atom in the hydroxyl species; White: hydrogen atom. (d) An alternative view of the $\text{La}(\text{OH})_3$ supercell.

The above figure shows the relaxed structures used in our first principles predictions of the O 1s binding energies. The primitive unit cells of the bulk structures of La_2O_3 , $\text{La}_2\text{O}_2\text{CO}_3$, and $\text{La}(\text{OH})_3$ are first relaxed, and the relaxed structures are then used to build the (3x3x2) supercell for bulk La_2O_3 , the (2x2x1) supercell for bulk $\text{La}_2\text{O}_2\text{CO}_3$, and the (2x2x3) supercell for bulk $\text{La}(\text{OH})_3$. These supercells are sufficiently large, which are required for the reliable predictions of the O 1s binding energies. A Γ -centered Monkhorst-Pack⁴ k-point mesh of (2x2x2) is used in these calculations.

The O 1s binding energies are usually calculated using the Δ SCF method with a well-defined reference, here the experimental value of 529.8 eV for the surface lattice oxygen site of the *in situ* prepared La₂O₃ sample, which is assigned to the La₂O₃ (001) surface due to its stability. The 1s binding energies for other types of oxygen sites are then calculated from

$$O_{1s} = \Delta O_{1s} + O_{1s}^{ref,exp} \quad (1)$$

where $O_{1s}^{ref,exp}$ is the reference O_{1s} binding energy, here 529.8 eV for the surface lattice oxygen on the La₂O₃ (001) surface, and ΔO_{1s} is calculated from

$$\Delta O_{1s} = (E_f - E_0) - (E_f^{ref} - E_0^{ref}) \quad (2)$$

where E_f and E_0 are the electronic energies of the system of interest with and without a core hole on the probed O atom, respectively (i.e. the final and initial states during the core hole formation). E_f calculation use a special pseudopotential with a core hole on the ionized atom. The superscript *ref* denotes the values for the reference.

Table S1. XPS peaks parameters: binding energy, FWHM value and La 3d_{5/2} spectral component separation. Energy scale is calibrated to La 4d_{5/2} peak maximum, 102.2 eV.

Sample	Binding energy, eV (FWHM, eV)			Δ La 3d, eV
	C 1s	O 1s	La 3d _{5/2}	
as prepared	284.5 (1.6) 285.9 (1.6) 287.9 (1.6) 289.5 (1.7)	528.5 (1.2) 531.0 (1.9) 532.3 (1.9)	835.2, 838.8	3.6
clean La ₂ O ₃	285.9 (2.1) 287.9 (2.3) 290.6 (2.3)	529.9 (1.3) 531.5 (2.4)	834.8, 839.1	4.3
O ₂ treated	286.1 (2.2) 287.7 (2.2) 290.1 (2.6)	529.8 (1.4) 531.7 (2.7) 533.5 (2.3)	834.5, 839.1	4.6
CO ₂ treated	286.2 (2.5) 288.3 (2.5) 290.6 (1.5) 291.9 (1.5)	529.7 (1.4) 530.7 (1.4) 532.6 (2.6)	834.6, 839.0	4.4
CH ₄ treated	284.9 (1.3) 286.0 (1.4) 287.4 (2.1)	529.9 (1.2) 531.4 (2.0)	834.4, 839.1	4.7
H ₂ O treated	286.2 (2.5) 288.4 (1.5) 290.6 (1.7)	529.8 (1.2) 531.8 (2.6)	835.6, 839.4	3.8

References

- (1) Liu, Z.; Ho Li, J. P.; Vovk, E.; Zhu, Y.; Li, S.; Wang, S.; van Bavel, A. P.; Yang, Y. Online Kinetics Study of Oxidative Coupling of Methane over La₂O₃ for Methane Activation: What Is Behind the Distinguished Light-off Temperatures? *ACS Catalysis* **2018**, 11761-11772.
- (2) Chen, G.; Han, B.; Deng, S.; Wang, Y.; Wang, Y. Lanthanum Dioxide Carbonate La₂O₂CO₃ Nanorods as a Sensing Material for Chemoresistive CO₂ Gas Sensor *Electrochim. Acta* **2014**, 127, 355-361.
- (3) Mu, Q.; Wang, Y. Synthesis, characterization, shape-preserved transformation, and optical properties of La(OH)₃, La₂O₂CO₃, and La₂O₃ nanorods *J. Alloys Compd.* **2011**, 509 (2), 396-401.
- (4) Monkhorst, H. J.; Pack, J. D. Special points for Brillouin-zone integrations *Phys. Rev. B* **1976**, 13 (12), 5188-5192.
- (5) www.quantum-espresso.org/upf_files/O.star1s-pbe-van_gipaw.UPF
- (6) Gougoussis, C.; Calandra, M.; Seitsonen, A. P.; Mauri, F.; *Phys. Rev. B* **2009**, 80, 075102